Research paper

N-donor ligands-directed coordination of Zn- azido complexes

Jing-Wen Wang, Chen Chen, Yao-Ja Li, Yang-Hui Luo, Bai-Wang Sun

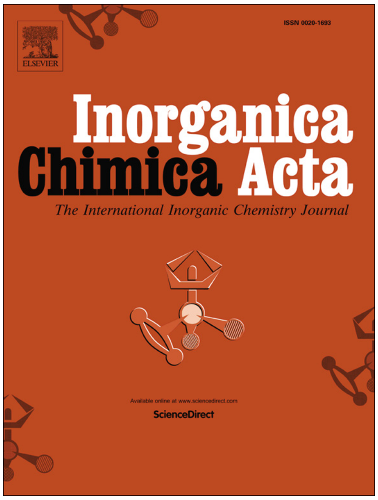

PII: S0020-1693(17)31006-X
DOI: https://doi.org/10.1016/j.ica.2017.09.064
Reference: ICA 17923

To appear in: *Inorganica Chimica Acta*

Received Date: 28 June 2017
Revised Date: 19 August 2017
Accepted Date: 29 September 2017

Please cite this article as: J-W. Wang, C. Chen, Y-J. Li, Y-H. Luo, B-W. Sun, N-donor ligands-directed coordination of Zn- azido complexes, *Inorganica Chimica Acta* (2017), doi: https://doi.org/10.1016/j.ica.2017.09.064

N-donor ligands-directed coordination of Zn- azido complexes

Jing-Wen Wang, Chen Chen, Yao-Ja Li, Yang-Hui Luo*, Bai-Wang Sun*

School of Chemistry and Chemical Engineering, Southeast University, Nanjing 211189, P. R. China

*E-mail: peluoyh@sina.com (Luo); chmsunbw@seu.edu.cn (Sun); Fax: +86-25-52090614; Tel：+86-25-52090614.

Abstract two zinc (II) pseudo-halide complexes $[Zn(L_1)(N_3)_2]_n$ (**1** L_1: 1,2-diaminocyclohexane) and $Zn(L_2)_2(N_3)_2$ (**2** L_2: 4,5-dimethy-2-(pyridine-2-yl) imidazole) have been synthesized and characterized. Single-crystal X-ray structural analysis revealed that the central Zn^{II} atoms in **1** displays distorted trigonal bipyramidal arrangement with a 1D chain structure bridged by N_3^- anions, while in **2**, the central Zn^{II} atoms incorporating with two bidentate L_2 ligands, and adopts an octahedral geometry and shows a "butterfly" coordination framework. Structural analysis demonstrated that the organic ligands play an important role in determining the resultant structure. In addition, both complexes were further characterized by thermal stability properties and Hirshfeld surface analysis.

Keywords Crystal structure; Coordination polymer; N-donor ligands; azido.

1 Introduction

Over the past years, coordination polymers (CPs) and metal-organic frameworks (MOFs) are the subjects of great interest due to their intriguing variety of topologies and structures as well as their enormous potential in many fields, such as magnets, ion-exchange, heterogeneous catalysts, chemical sensing, luminescence and gas storage [1-7]. Despite the remarkable achievements reached in this aspect so far, the rational control in the construction of coordination frameworks remains a considerable challenge at this stage and much more work is required to extend the knowledge in this field [8-11]. To a certain degree, the final structures of coordination polymers and metal-organic frameworks can be reasonably controlled and directed by combination of various forces such as metal-ligand coordination bond and much weaker interactions [12-14].

In addition, several factors including metals atoms, temperature, the organic anions and N-donor ligands can affect the final structures of coordination polymers and metal-organic frameworks [15-18]. Taking into account the various factors, the choice of the organic ligand is a key factor that affects the construction of coordination compounds with interesting structures [19, 20]. Besides, the skillful introduction of co-ligands into the self-assembly process can also result in completely different structural motifs [10, 21]. Organic N-heterocycle ligands are good building blocks for the construction of coordination polymers or metal-organic frameworks, beacuse amino groups and multidentate chelating aromatic nitrogen atoms have an excellent coordination capability and versatile coordination modes [22-24]. Among them, imidazole derivatives are regarded as interesting ligands, because they can adopt different conformations according to the geometric needs of the different metal ions [24]. On the other hand, cleavage of the sp^3C-N bond in cyclohexylamine (87.6 kcal $mol^{-1})^2$ is relatively facile [23], so it can be used as an excellent multi-functional ligand for the construction of coordination polymers [25-27]. Additionally, in our previous work, the effect of pseudohalide anions (SCN^- and $SeCN^-$) on the spin-crossover of SCO systems was proof and the multidendate 4,5-dimethy-2 -(pyridine-2-yl)imidazole was selected as organic ligand to react with $Fe(ClO_4)_2$[28, 29].

Taking inspiration from the points mentioned above, we explored organic aromatic ligand 4,5-dimethy-2-(pyridine-2-yl)imidazole as organic ligand (L_2), pseudohalide (N_3^-) were selected as co-ligands, beside, saturated N-heterocyclic ligand 1, 2-cyclohexanediamine, which can adopt various coordination modes to bind metal centers of specific coordination geometry, is employed as another comparative organic ligand, to react with $Zn(NO_3)_2$, aiming to further investigate the influence of different types of organic ligands on the structures and properties of coordination compounds. As expected, two new complexes have been obtained $[Zn (L_1)(N_3)_2]_n$ (**1**) and $Zn(L_2)_2(N_3)$ (**2**) (Scheme 1). Single-crystal X-ray diffraction results revealed that the **1** displays a 1D chain polymer with five-coordinated trigonal bipyramidal arrangement while **2** is in six-coordinated octahedral geometry. TGA, PXRD and Hirshfeld Surface also were performed.

2 Results and discussion

2.1.1 Crystal Structure of Complex 1

The asymmetric coordination unit of complex **1** composed of one central Zn^{II} ion, one L_1 ligand and two N_3^- ions. As can be seen in Figure 1b, the each central Zn^{II} ion is five-coordinated in a distorted trigonal bipyramidal environment with five N atoms, two from L_1 ligands [Zn1-N2: 2.078(2) and Zn1-N1 2.019(3) Å] and three from N_3^- ligands [Zn1-N6: 2.237(3) Å, Zn1-N8= 2.306(3) Å, Zn1-N3: 1.974(3) Å]. Where, the axial positions are occupied by N1, N2 and N3 with the N1-Zn1-N3 bond angle of 137.14 (2), N2-Zn1-N3 bond angle of 136.21 (3) and the equatorial mean plane is slightly distorted with N6-Zn1-N8 bond angle of 175.34 (19). The L_1 ligand behaves as the bidentate ligand via two amino groups, and N_3^- co-ligands bridge the adjacent central Zn^{II} ions affording a 1D chain structure with the Zn···Zn distance of

6.310(1)Å (Figure 1b). The N_3^- anions use two different types of bridging modes. One N_3^- behaves as the terminal ligand, adopting the EO-bridged azide pairs binding mode; the other N_3^- behaves as the EE-bridged azides with N6-Zn-N8 into an infinited 1D chains forming a coordination polymer, additionally, these adjacent 1D chains are further connected via N-H···N hydrogen bonding interaction between coordinated amino group of L_1 ligand and the uncoordinated N atoms of N_3^- ions as well as C-H···C weak interaction to resulting in 3D layered structure (Fig. 1c).

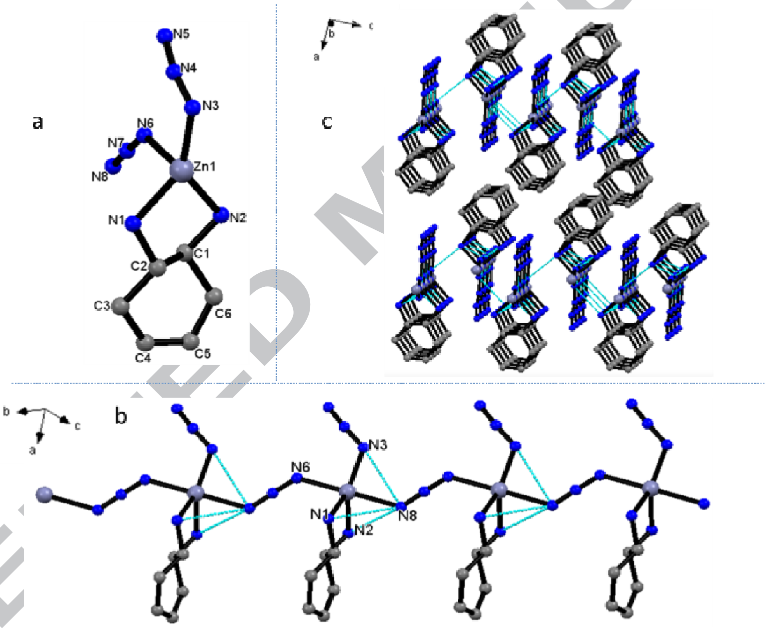

Figure 1 (a) The asymmetric unit of compounds **1.** (b) 1D chain diagram of compound **1**. (c) The crystal packing of compound **1** viewed along the b-axis and the intermolecular hydrogen bond interactions have been marked. Hydrogen atoms are omitted for clarity.

Table 2 Selected bond lengths (Å) and angles (°) for complexes **1** and **2**

1	**1**	**2**	**2**
Zn1-N1	2.038	Zn1-N1	1.964
Zn1-N2	2.089	Zn1-N2	1.951
Zn1-N3	1.971	Zn1-N4	2.004
Zn1-N6	2.248	Zn1-N5	1.970
N1-H-N5	3.350	Zn1-N7	1.941
		Zn1-N9	1.969
Mean	2.0865		1.9665
N1-Zn1-N2	86.15	N1-Zn1-N2	83.15
N1-Zn1-N3	138.33	N7-Zn1-N4	88.75
N2-Zn1-N6	92.69	N7-Zn1-N5	170.03
N3-Zn1-N6	90.81	N2-Zn1-N9	173.84
		N5-Zn1-N9	88.37
		N1-Zn1-N4	177.30

2.1.2 Crystal Structure of Complex 2

Complex **2** crystallizes as colorless block crystals in the orthorhombic Pbcn space group, the asymmetric unit (ASU) consisting of a Zn^{II} ion, two N_3^- ions, and two ligands L_2 (Figure 2a) displays a "batterfly-like" motif. In the crystal, each Zn^{II} ion adopts a distorted six-coordinated in an octahedral geometry surrounded by four N atoms originating from ligands L_2 liking two wings and two N atoms from N_3^- ions which just similar to two antennae. Every "batterfly" motif packed into 1D chains through N3···N6 solitary electrons contacts (Fig. 1b), and the 1D chains then stacked into 3D motif (Fig. 1c) by C-H···π and π···π weaker interactions. For the "batterfly-like" unit, the average Zn-N distance is 1.9665 Å (Table 2) which is significantly shorter than which has been reported complexes [10, 30]. Besides, the N_3^- ion is almost linear [N7-N8-N20, 177.47(7)], whereas the Zn-N-N (N) linkages are slightly bent [Zn1-N7-N8, 119.23(5)]. In addition, the selected bond distances and angles of complexes **1**, **2** are tabulated in Table 2 and geometrical parameters for hydrogen bonds are shown in Table 3.

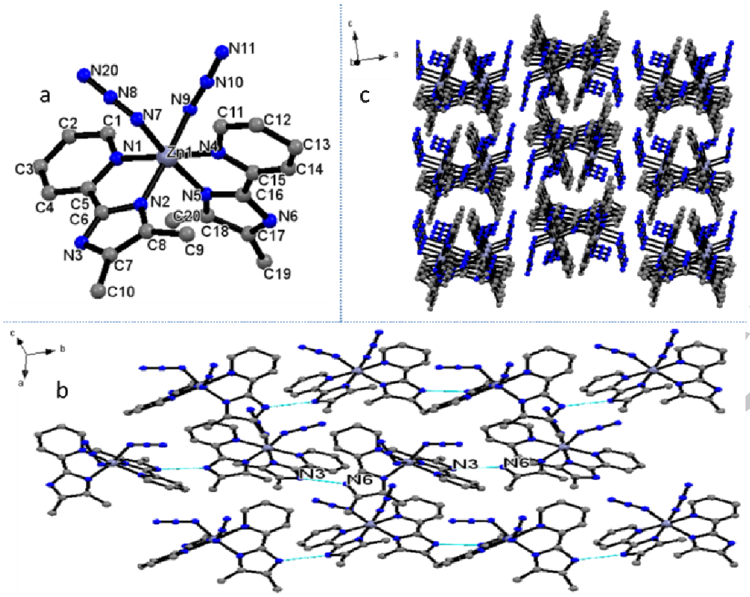

Figure 2. (a) The asymmetric unit of compounds **2**. (b) 1D chain diagram of compound **2** (c) The crystals packing of compound **2** viewed along the b-axis. Hydrogen atoms are omitted for clarity.

2.1.3 Structural Discussion of Complexes 1 and 2

Complexes **1** and **2** were obtained via the assembly of $Zn(NO_3)_2$ and azido (N_3^-) with the presence of ligand *L₁*, *L₂* respectively, affording different coordination modes and supramolecular lattices, coordination polymers (CPs) and metal-organic frameworks (MOFs), respectively. In complexes, the central Zn^{II} ion adopts five- and six-coordinated forming two different distorted arrangement, trigonal bipyramidal and octahedral geometry, for compounds **1**, **2**, resulting from the different N-heterocycles donor organic ligands which L_1 belongs to saturated, whereas L_2 is a part of aromatic compounds. It implies the saturation of N-donor ligands can influence coordination modes of compounds. Besides, it should be noted that the N_3^- anions represent two kinds of binding modes (EO and EE bridged model) in **1** and only adopts EO bridged model forming the monodentate coordination fashions in **2**. As a result, compound **1** shows an infinite 1D coordination polymer and **2** displays mononuclear metal-organic framework compound. These structural distinguish may be ascribed to the distinct coordination ability and steric bulk of the N-heterocyclic ligands (L_1 and L_2).

Table 3 Geometrical parameters for the hydrogen bonds in compounds **1** and **2**.

D-H···A	D···A(Å)	H···A(Å)	∠D-H···A(°)	Symmetry operation
Compound **1**				
N1-H1A···N5	3.411	2.622	148.29	3/2-x, -1/2+y, -1/2+z
N1-H1A···N6	3.084	2.422	131.44	3/2-x, -1/2+y, -1/2+z
N1-H1B···N3	3.141	2.310	155.47	3/2-x, 1/2+y, -1/2+z
N2-H2A···N3	3.171	2.298	167.06	3/2-x, 1/2+y, 1/2+z
N2-H2B···N5	3.448	2.597	160.26	3/2-x, -1/2+y, 1/2+z
Compound **2**				
C1-H1···N20	3.376	2.735	126.82	
C10-H10A···N11	3.534	2.634	156.29	

2.2 Hirshfeld Surface

Hirshfeld surface is a powerful tool for the identification of intermolecular interactions. The 3D dnorm values are mapped onto a red-blue-white color Hirshfeld surface and red regions represent closer contacts, blue regions represent longer contacts and white regions represent the distance of contacts which is exactly the vdW separation. What is more, the 3D dnorm can be converted into 2D fingerprint plots, which we can analysis the intermolecular contacts and get a quantitative summary of the nature and type of intermolecular contacts [31, 32].

The 3D Hirshfeld surface (dnorm) and 2D fingerprint plots of complex **1** and **2** are shown in Figure 3. In complex **1**, the red regions on the dnorm surface represent the significant N-H···N hydrogen bonding interactions, which represent the closest

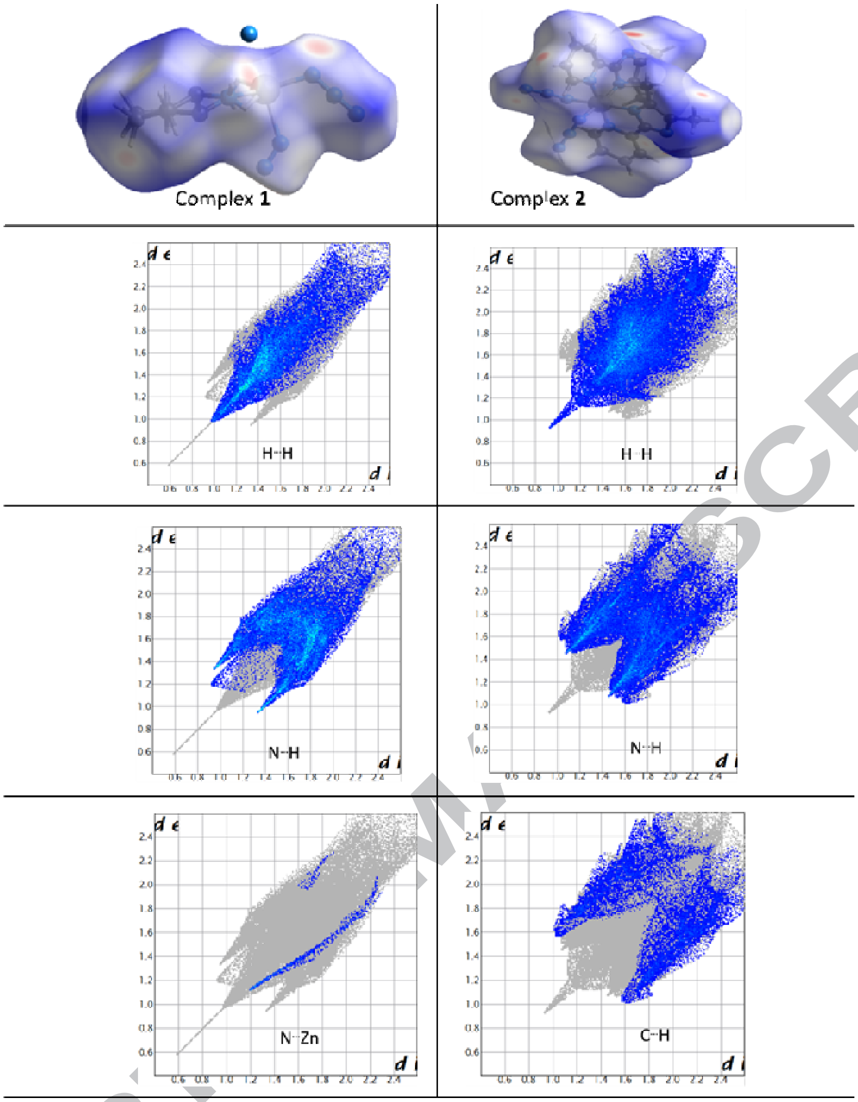

Figure. 3 3D molecular Hirshfeld dnorm surfaces and 2D fingerprint plots of complexes **1** and **2**.

intermolecular interactions in the crystal. The small red points on the dnorm surfaces are corresponding to the significant N4-Zn interaction, which due to the close approach of an N atom of azide anion to the central Zn^{II} ion. And the blue regions represent the H···H interactions. Obviously, the blue regions occupy the most of Hirshfeld surface about 35.8% to the total Hirshfeld surfaces. Actually, the proportion of N-H···N and N···Zn interaction calculated by two-dimensional (2D) fingerprint plot are found to be 47.3%, and 1.8% to the total Hirshfeld surfaces of complex **1**, which is consistent with the analysis of the crystal structure. In complex **2**, the larger red regions on the upper right and bottom right of the dnorm surfaces are corresponding to the C-H···N weak hydrogen bonding and N···N interactions which have a great significant contribution to the total Hirshfeld surfaces with comprise of 36.4%, 2.2%, respectively, to the total Hirshfeld surfaces. Interestingly, N···Zn interactions are found only in compound **1**, and C···H intermolecular interactions exist only in compound **2.** These differences of the interaction in the crystal structures of compounds **1**, **2** also are clearly shown in Fig. 1 and Fig. 2. Apart from those above, the presence of H···H, N···N and C···N intermolecular interactions are observed, and the percentages of them are summarized in Fig. 4.

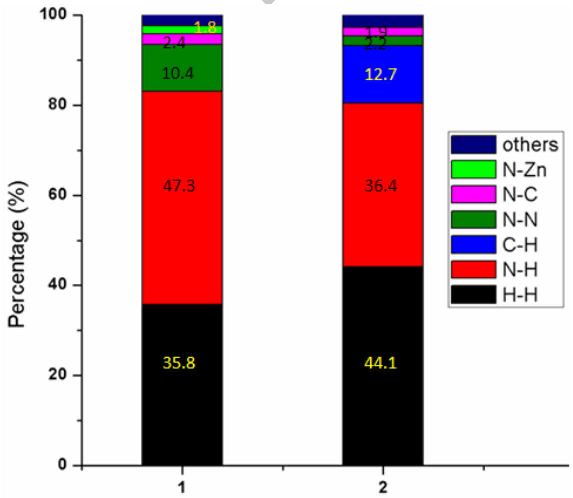

Figure. 4 Percentage contributions from individual intermolecular interactions to the Hirshfeld surfaces of complexes **1** and **2.**

2.3 Thermal Study

The thermal behaviors of complexes L_1 and L_2 are investigated on a Proteus Thermal analyse system (from NETZSCH TG 2009 F3) and the heating rate is around 20 K min^{-1} with the temperature range of 30-600℃. Figure 5 shows the TGA traces of them. For complex **1,** the complex keeps stable up to 292 °C and then suffers a sharp weight loss until heating to 330 °C, which is due to the decomposition of the ligands with mass loss of 38.52% (the calculated ratio is 42.48%) to give the $Zn(N_3)_2$ residue. With regard to complex **2**, the thermal profile of **2** is different from the **1**, the abrupt weight loss of the main framework occurs from 359 °C, by the mass decomposition of two ligands about 70.38% (the calculated ratio is 69.83%). In addition, the phase purities of the complexes are also identified by PXRD patterns, which show the essential difference to diverse central Zn^{II} ion distorted arrangement (Figure. 6).

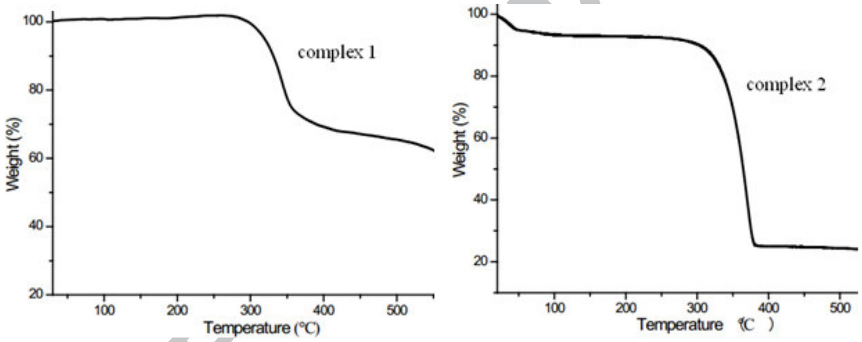

Figure. 5 TGA profiles of compounds **1**, **2** in the temperature range of 30-600℃.

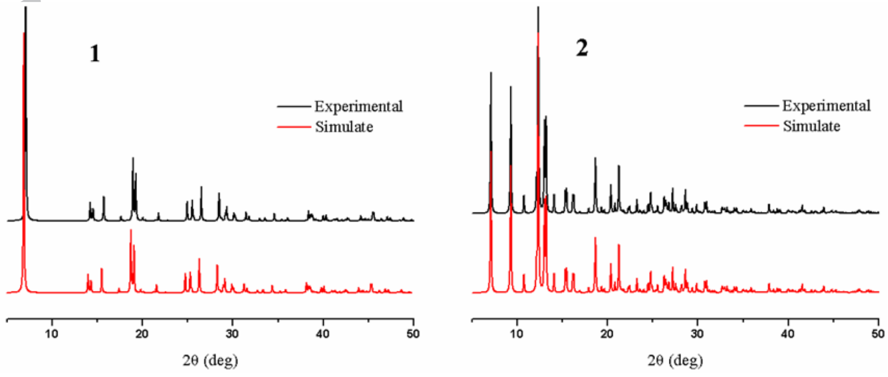

Fig. 6 Experimental and simulated PXRD patterns for both complexes

3 Conclusions

In summary, two new zinc (II) coordination complexes, $[Zn(L_1)(N_3)_2]_n$ (**1**) and $Zn(L_2)_2(N_3)_2$ (**2**), have been successfully synthesized and structurally characterized. Single-crystal X-ray analysis show structural diversity in both complexes essentially arising from the usage of different ligands resulting in different central Zn^{II} ion distorted arrangement, trigonal bipyramidal and octahedral geometry, respectively. In addition, complex **1** exhibits the characteristic Zn···N interaction. Systematic exploration of the significant ligands effect with other metal atoms as well as pseudo-halide ions is currently underway and this work will contribute to further insights in the rational design of coordination complexes.

4 Experimental

4.1 Materials and physical measurements

All reagents were obtained commercially, and used without further purification. thermogravimetric analysis (TGA) was performed using a NETZSCH TG 2009 F3 system at a heating rate of 20 K min^{-1} under an atmosphere of dry nitrogen flowing at 20 $cm^3 min^{-1}$ over the range from 50 to 600℃. Elemental analyses for carbon, hydrogen and nitrogen were performed using a Vario-EL III elemental analyzer. X-ray powder diffraction was recorded on a D8 ADVANCE XRD (Bruker, Germany) with Cu Kα radiation (λ = 1.54056 Å) at 40 mA and 45 kV. The sample was packed into a glass holder and diffraction patterns were collected over a 2θ range of 5-50, at a scan rate of 3° min^{-1}.

4.2 Synthesis of *L_2* (4,5-dimethy-2-(pyridine-2-yl)imidazole).

The synthetic routes of the ligand *L_2* are illustrated in Scheme 1 [28]. 1 ml oxalylchloride (10 mmol) was added dropwise to a CH_2Cl_2 solution (100 ml) with 1.5 g N-methylacetamide (20 mmol) at 0℃ under heavy gas evolution. After stirred for about 30 min, 2-pyridine carboxamide (2.74 g, 10 mmol) was added. The obtained mixture was stirred for 3h at rt, and the volatiles were removed under reduced pressure. The residue was dissolved in an aqueous solution of $NaHCO_3$ (60 ml) and refluxed for a further 2 h at 100 ℃. The water phase was extracted three times with $CHCl_3$. The organic phase was concentrated and re-crystallized from MeOH gave the ligand *L_2*. Yield: 1.14 g, ca. 78%. Elemental analysis (%) for *L_2* ($C_{10}H_{11}N_3$): Calc.: C, 69.34; H, 6.40; N, 24.25; found: C, 69.27; H, 6.44; N, 24.19%. IR (KBr, cm1): 3048, 2980, 2180, 1750, 1560, 1562, 1533, 1482, 1340, 1269, 1235, 1120, 1040, 1015, 987, 960, 798, 747, 721. ^{1}H NMR d: 2.67-2.75 (d, 6H), 7.36 (m, H), 7.85 (m, 1H), 8.38 (d, 1H), 8.59 (d, 1H), 13.00 (s, 1H). ^{13}C NMR d: 12.6, 43.5, 124.5, 125.6, 131.6, 137.2, 143.4, 149.2, 155.1, 165.9.

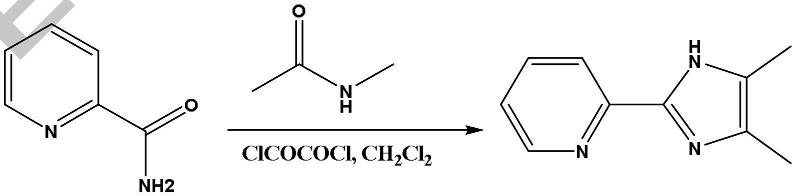

Scheme 1. The synthetic route for ligand *L_2*.

4.3 Synthesis of complexes 1 and 2.

To a solution of $Zn(NO_3)_2·6H_2O$ (0.4 mmol) in MeOH (10 mL), a solution of ligand *L_1* (0.8 mmol) in MeOH (10 mL) was added. The mixture was added into an aqueous solution containing NaN_3 (0.8 mmol) under continuous stirring (Scheme 2). After stirring for about 30 min, the solution which results from the mixture was filtered off and allowed to evaporate at room temperature. Crystals suitable for X-ray single-crystal diffraction or PXRD were obtained within two weeks and collected by filtration. Yield: ca. 85%. Elemental analysis (%) for **1** ($C_6H_{14}N_8Zn$): Calc.: C, 27.33; H, 0.38; N, 42.51; found: C, 27.43; H, 0.78; N, 42.52%. Complex **2** is synthesized using a similar method ($C_{20}H_{20}N_{12}Zn$): Calc.: C, 48.63; H, 4.08; N, 34.04; found: C, 48.65; H, 4.10; N, 34.24%.

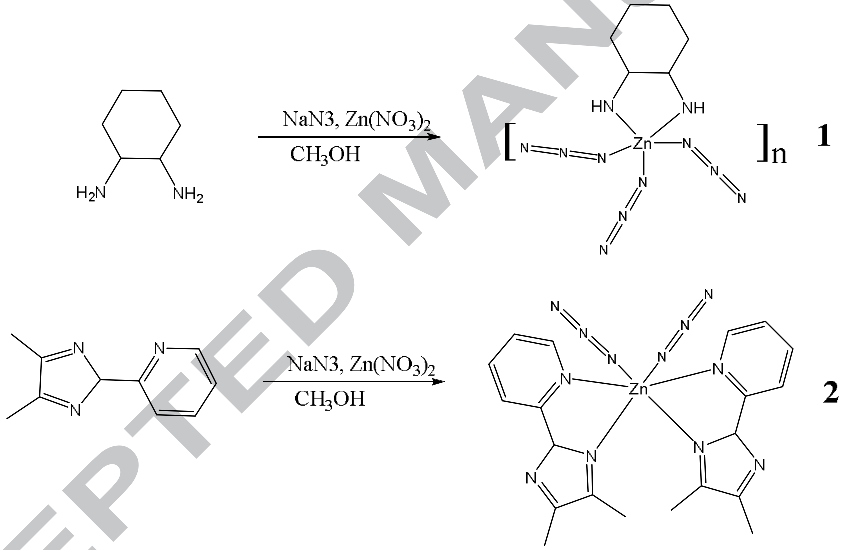

Scheme 2. The synthetic route for complexes **1** and **2**.

4.4 X-ray crystallographic study

The single-crystal X-ray diffraction data of complexes **1** and **2** were collected with graphite-monochromated Mo Ka radiation (λ= 0.071073 nm). A Rigaku SCXmini diffractometer with the v-scan technique was used [33，34]. The lattice parameters were integrated using vector analysis and refined from the diffraction matrix, the absorption correction was carried out by using Bruker SADABS program with the multi-scan method. The structures were solved by full-matrix least-squares methods on all F^2 data. The SHELXS-2014 and SHELXL-2014 programs [35] were used for structure solution and structure refinement, respectively. The molecular graphics were prepared by using the mercury program [36].

Table 1 Crystal data and structure refinement for compounds **1**, **2**.

Molecular salts	**1**	**2**
Formula	$C_6H_{14}N_8Zn$	$C_{20}H_{20}N_{12}Zn$
Formula weight	263.63	493.85
Crystal system	orthorhombic	orthorhombic
Space group	$Pna2_1$	Pbcn
a/ Å	24.882(5)	19.000(2)
b/ Å	6.3101(13)	16.4176(18)
c/ Å	6.9762(14)	14.5330(16)
V, Å^3	1095.3(4)	4533.5(9)
Z	4	8
D calc (Mg m^{-3})	1.586	1.447
T/K	293(2)	293(2)
μ (mm^{-1})	2.225	1.796
Cryst dimensions	0.2×0.25×0.32	0.3×0.25×0.2
No. of reflns collected	2480	3993
No. of unique reflns	1863	2102
No. of params	116	298
Goodness-of-fit on F^2	1.089	1.050
R1,wR2 ($I>2\sigma(I)$)	0.0579, 0.1378	0.1264, 0.3374
R1,wR2 (all data)	0.0812, 0.1505	0.1979, 0.3975
CCDC NO.	1557016	1557017

Note: due to the poor quality of crystal **2**, some of the data collected is not very good but this does not affect the final structure.

Acknowledgements

This research was based on work supported by the Natural Science Foundation of China (Grant Nos. 21371031 and 21628101), International S&T Cooperation Program of China (No. 2015DFG42240) and the Priority Academic Program Development (PAPD) of Jiangsu Higher Education Institutions.

References

[1] D.T. Genna, A.G. Wong-Foy, A.J. Matzger, M.S. Sanford, J. Am. Chem. Soc. 135 (2013) 10586.

[2] X.J. Xu, J Inorg Organomet Polym. 25 (2015) 606.

[3] N.N. Adarsh, P. Dastidar, Chem. Soc. Rev. 41 (2012) 3039.

[4] T.R. Cook, Y.R. Zheng, P.J. Stang, Chem. Rev. 113 (2013) 734.

[5] D.S. Li, Y.P. Wu, J. Zhao, J. Zhang, J.Y. Lu, Coord. Chem. Rev. 1 (2014) 1.

[6] C. Wang, T. Zhang, W. Lin, Chem. Rev. 112 (2012) 1084.

[7] M.Y. Li, F. Wang, J. Zhang, Inorganic Chemistry Communications 79 (2017) 37.

[8] G.C. Shearer, S. Chavan, S. Bordiga, S. Svelle, U. Olsbye, K.P. Lillerud, Chem. Mater. 28 (2016) 3749.

[9] J.A. Hua, Y. Zhao, D. Zhao, Y.S. Kang, K. Chen, W.Y. Sun, RSC Adv. 5 (2015) 43268.

[10] Q. Chen, Y. Bi, J. Chen, Z. Anorg. Allg. Chem. 642 (2016) 1445.

[11] M. Du, C.P. Li, C.S. Liu, S.M. Fang, Coord. Chem. Rev. 257 (2013) 1282.

[12] H.M. Zhang, Y.C. He, J. Yang, Y.Y. Liu, J.F. Ma, Cryst. Growth Des. 14 (2014) 2307.

[13] B.E. Partridge, P. Leowanawat, E. Aqad, M.R. Imam, H.J. Sun, M. Peterca, P.A. Heiney, R. Graf, H.W. Spiess, X. Zeng, G. Ungar, V. Percec, J. Am. Chem. Soc. 137 (2015) 5210.

[14] D. Aulakh, J.R. Varghese, M. Wriedt, Inorg. Chem. 54 (2015) 1756.

[15] G.Z. Liu, X.D. Li, X.L. Li, L.Y. Wang, CrystEngComm 15 (2013) 2428

[16] C.P. Li, M. Du, Chem. Commun. 47 (2011) 5958.

[17] H.R. Khavasi, B.M.M. Sadegh, Inorg. Chem. 49 (2010) 5356.

[18] Y. Garcia, N.N. Adarsh, A.D. Naik, Chimia 67 (2013) 411.

[19] R.M. Han, J.F. Ma, Y.Y. Liu, J. Yang, CrystEngComm 15 (2013) 5641.

[20] X.Wang, A.X. Tian, X.L. Wang, RSC Adv. 5 (2015) 41155.

[21] H.L. Sun, Z.M. Wang, S. Gao, Inorg. Chem. 44 (2005) 2169.

[22] (a) M.L. Han, S.-C. Wang, D.F. Feng, Cryst. Res. Technol. 49 (2014) 276;
(b) S. Mallik, R.D. Johnson, F.H. Arnold, J. Am. Chem. Soc. 116 (1994) 8902.

[23] M. Bachrach, T.J. Marks, J.M. Notestein, New J. Chem. 40 (2016) 6001.

[24] P. Zhang, B.Y. Guan, L. Yu, X.W. (David) Lou, Angew. Chem. Int. Ed. 56 (2017) 7141.

[25] K. Mnqiwu, T. Xaba, M.J. Moloto, P.K. Mubiayi, P. Nyamukamba, S.B. Sibokoza Materials Letters 199 (2017) 28.

[26] J. Wu, Y.Y. Pu, X.W. Zhao, L.W. Qian, G.Q. Bian, Q.Y. Zhu, J. Dai, Dalton Trans. 44 (2015) 4520.

[27] C. Li, X.F. Meng, W.N. Li, X. Zhou, J.J. Ma, Synthesis and Reactivity in Inorganic, Metal-Organic, and Nano-Metal Chemistry 46 (2016) 185.

[28] Y.H. Luo, L. Chen, J.W. Wang, M.X. Wang, Y.W. Zhang, B.W. Sun, Inorganica Chimica Acta 450 (2016) 8.

[29] Y.H. Luo, G.J. Wen, L.S. Gu, M.N. Wang, B.W. Sun, Polyhedron 121 (2017)

101.

[30] W.H. Jiang, J.L. Liu, L.Z. Niu, B. Liu, Y.H. Yu, G.F. Hou, D.S. Ma, Polyhedron 124 (2017) 191.

[31] (a)Y.-H. Luo, C. Chen, Y.-J. Li, J.-W. Wang, B.-W. Sun, Dyes and Pigments 143 (2017) 239;

(b) Y.H. Luo, J.W. Wang, C. Chen, Y.J. Li, B.W. Sun, Cryst. Growth Des. 17 (2017) 2576.

[32] J.-W. Wang, Y.-W. Zhang, M.-X. Wang, Y.-H. Luo, B.-W. Sun, Polyhedron 124 (2017) 243.

[33] Yarnton, Oxfordshire. Agilent Technologies (formerly Oxford Diffraction). England, 2012.

[34] (a)Y.H. Luo, L.J. Yang, Q.L. Liu, Y. Ling, Y. Sun, J.W. Wang, C.Q. You, B.W. Sun, J. Mater. Chem. C. 4 (2016) 8061;

(b) Y.H. Luo, M. Nihei, G.J. Wen, B.W. Sun, H. Oshio, Inorg. Chem. 55 (2016) 8147.

[35] (a) G.M. Sheldrick, Acta Crystallogr, 3 (2015) C71;

(b) Rigaku, CrystalClear, Version 14.0. Rigaku Corporation. Tokyo, Japan, 2005.

[36] Mercury 2.3 Supplied with Cambridge Structural Database, CCDC, Cambridge, U.K., 2003-2004

Highlights

- The connecting motif of two different organic ligands have been characterized;
- The influence of ligands on the structure of complexes with N_3^- anions has been demonstrated;
- The connecting types N_3^- anions have been classified.

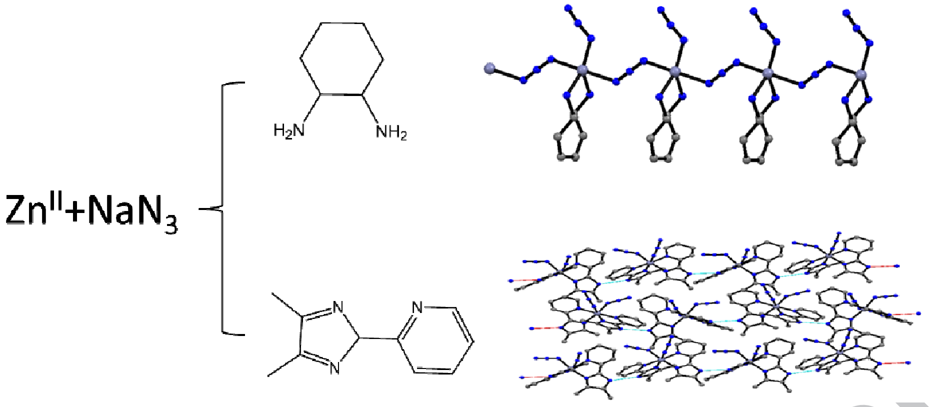

The influences of organic ligands with different binding motifs on the structures and properties of coordination compounds with Zn ^{II} and N_3^- anions have been demonstrated.